Alam, A.K.M.B., Niioka, M., Fukuda, D. and Fujii, Y. (2013), Confining Pressure Effect on Structual Changes in Rock Types under Consolidation and Compression, Proc. MMIJ Fall Meeting 2013 Sapporo, PY-7, p. 571, Hokkaido University, Sapporo, Sep. 3

Confining Pressure Effect on Structural Changes in Rock Types under Consolidation and Compression

Alam AKM B., Niioka M., Fukuda D., Fujii Y., Hokkaido Univ.

Triaxial tests were carried out at 1–15 MPa confining pressures (CP) at 295 K. The samples of 30 mm diameter and 60 mm in length were held for 24 h at the target consolidation pressure, and then constant strain-rate compression at 10^{-5} s^{-1} was applied until the stroke-based strain reached 10 % for the Shikotsu welded tuff or 7 % for the Kimachi sandstone and Inada granite. After the tests, microstructure was analyzed by thin-section image analysis (TSIA) with a resolution of 8.8 µm of the blue resin-impregnated specimens, and macrostructure (the number, orientation, and geometry of the rupture planes of the specimens) was also analyzed by micro-focus X-ray computed tomography (CT) with a resolution of 37 µm.

For Shikotsu welded tuff, the porosity decreased by 41.23 % due to the consolidation at 15 MPa CP by TSIA. This occurred because the CP was close to the unconfined compressive strength and was sufficiently high to cause pore collapse. The equivalent diameter of pores (d_{pore}) in the intact specimen was 0.04–0.16 mm. The frequency of $d_{pore} \geq 0.08$ mm decreased, and $d_{pore} \leq 0.08$ mm became dominant at 15 MPa CP (Fig. 1). Pores with a smaller aspect ratio increased at 15 MPa CP, but pores with a small angle to the horizontal flow layer remained dominant in the 15 MPa-consolidated specimen. A rupture plane was observed in the CT images in axial plane of the specimen after axial compression at 1 MPa CP. However, macroscopic fractures were not observed for 15 MPa CP. The porosity by TSIA near the rupture plane after axial compression at 1 MPa CP increased by 16.99% and was greater than that far from the rupture plane. The frequency value of d_{pore} = 0.10 mm increased near the rupture plane, and the frequency value of d_{pore} = 0.06 mm was dominant far from the rupture plane. The frequency of a pore aspect ratio of around 0.5 decreased near the rupture plane.

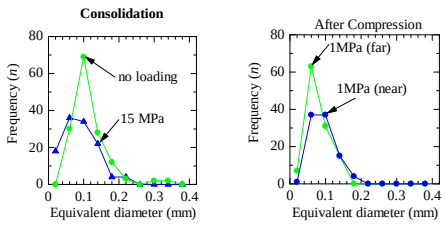

Fig. 1 Equivalent diameter of pores of Shikotsu welded tuff.

For Kimachi sandstone, the 0.39 mm average thickness of cementing materials by TSIA for 1 MPa CP consolidation was much thicker than the 0.25 mm average by compaction at 15 MPa CP. A distinct main rupture plane was observed in the CT images after axial compression at 1 MPa CP (Fig. 2a). Several subrupture planes were observed and the thickness of cementing materials was 0.27 mm. At 7 MPa CP, only one main rupture plane was found. At 15 MPa CP, macroscopic rupture planes were observed neither in CT images (Fig. 2b) nor in TSIA. This occurred because large plastic deformation took place in the cementing materials. The thickness of the cementing materials was 0.20 mm.

(a) (b)

Fig. 2 Sample and CT images of Kimachi sandstone under compression (a) at 1 MPa CP (b) at 15 MPa CP.

For Inada granite, no consolidation effect was observed in TSIA. A main rupture plane in the axial plane, with subrupture planes, was observed in the CT image at 1 MPa CP (Fig. 3a). The main rupture plane consisted of a network of microcracks. Numerous axial cracks from biotite grains were also observed. The distinct single rupture plane in the CT image was also observed in TSIA at 9 MPa CP. This rupture plane also consisted of a network of microcracks; however, it had a smaller width than that at 1 MPa CP, and axial cracks from biotite were not observed. Multiple rupture planes were observed at 15 MPa CP (Fig. 3b). The subrupture planes formed, as there were no soft cementing materials between mineral grains, so significant stress concentration occurred on the stiff and rough main rupture plane.

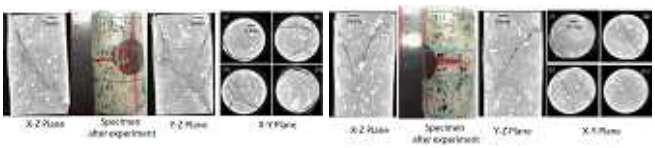

(a) (b)

Fig. 3 Sample and CT images of Inada granite under compression (a) at 1 MPa CP (b) at 15 MPa CP.